Desalination 565 (2023) 116846

Contents lists available at ScienceDirect

Desalination

journal homepage: www.elsevier.com/locate/desal

Behavior and removal of microplastics during desalination in a lab-scale direct contact membrane distillation system

Mariana N. Miranda, A. Rita T. Fernandes, Adrián M.T. Silva *, M. Fernando R. Pereira

LSRE-LCM - Laboratory of Separation and Reaction Engineering - Laboratory of Catalysis and Materials, Faculty of Engineering, University of Porto, Rua Dr. Roberto Frias, 4200-465 Porto, Portugal
ALiCE - Associate Laboratory in Chemical Engineering, Faculty of Engineering, University of Porto, Rua Dr. Roberto Frias, 4200-465 Porto, Portugal

HIGHLIGHTS

- Pioneer study of microplastics behavior and removal in membrane distillation
- μRaman hints DCMD high removal efficiency (≥ 99 %) of microplastics from seawater
- Microplastics loads >0.1 g L^{-1} can lead to a decrease in the DCMD performance
- Low aging of uPVC during an 8 h desalination process in a DCMD lab-scale system
- uPVC developed a pink coloration during temperature stress batch experiments

GRAPHICAL ABSTRACT

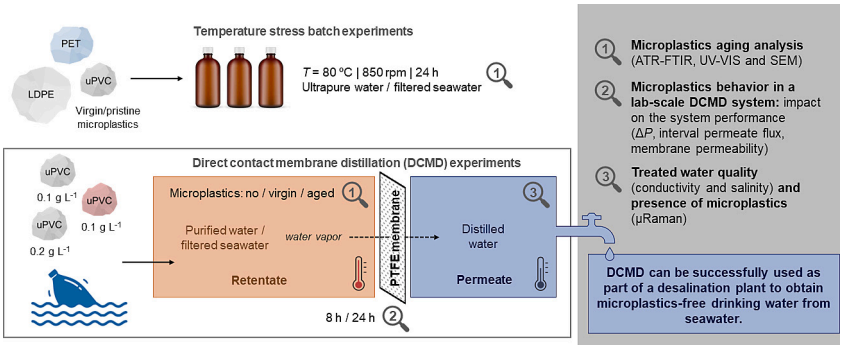

ARTICLE INFO

Keywords:
Aging
Drinking water
Membrane distillation
Microplastics
Seawater

ABSTRACT

The behavior of microplastic particles (MPPs) is explored in a lab-scale direct contact membrane distillation (DCMD) system used to produce drinking water from seawater, while also analyzing the impact of their presence on the process performance. Commercial MPPs (LDPE, PET and uPVC) were first studied by temperature stress (TS) tests (using amber bottles) to mimic the exposure to the high temperatures commonly used in DCMD (ca. 80 °C), which led to uPVC being selected to be tested under different loads and aging degrees in the DCMD system. By analyzing uPVC MPPs samples before and after the TS and DCMD experiments by ATR-FTIR, UV–Visible spectroscopy and SEM, it was concluded that minor aging is expected to occur. High loads (>0.1 g L^{-1}) of uPVC MPPs decreased the DCMD performance in terms of permeate flux (from 32.8 ± 0.3 with filtered seawater to 28.7 ± 0.3 kg m^{-2} h^{-1} with a load of 0.2 g L^{-1}), although no signs of inferior treated water quality were found based on the conductivity and salinity results. The removal of MPPs (size > 1.2 μm) in DCMD applications with seawater was analyzed by μRaman, with all the results suggesting very high removal efficiencies (≥99 %).

* Corresponding author at: LSRE-LCM - Laboratory of Separation and Reaction Engineering - Laboratory of Catalysis and Materials, Faculty of Engineering, University of Porto, Rua Dr. Roberto Frias, 4200-465 Porto, Portugal.
E-mail address: adrian@fe.up.pt (A.M.T. Silva).

https://doi.org/10.1016/j.desal.2023.116846
Received 4 May 2023; Received in revised form 4 July 2023; Accepted 15 July 2023
Available online 18 July 2023

1. Introduction

Although the risk of microplastics and nanoplastics to human health is yet to be established [1,2], the growing amount of reports related to the detection of plastics in food [3,4], beverages [5,6], air dust [7,8] and on human tissue and biological samples [9–11] has been rising concern to their potential toxicological impacts to our species [12]. In particular, the microplastics presence in drinking water is of major importance due to its universal and daily consumption.

The World Health Organization (WHO) identified several data gaps and the highest priority research needs regarding this topic, which include the development of standard methods for microplastics sampling and analysis, more studies on the occurrence and characteristics of microplastics in drinking water, and more data that have to be obtained on the occurrence and fate of microplastics throughout the water supply chain [13]. This last research need calls for the analysis of microplastics behavior in the water supply chain, the effectiveness of the water treatments applied, and the microplastics occurrence from the source of raw water to the distribution system or bottling.

Since then, several studies have been published in line with those needs, especially focused on drinking water treatment plants (DWTPs), pipe distribution systems [14] and bottled and tap drinking water obtained from surface freshwater or groundwater sources, with seawater receiving far less attention [15,16]. The most common technologies for the removal of particulate matter and/or organic matter have been reviewed and include coagulation-flocculation and sedimentation, membrane filtration (ultrafiltration, microfiltration and reverse osmosis), and media filtration (sand and granular activated carbon) [16,17]. These studies demonstrate that conventional and advanced DWTPs can remove most of the microplastics from water, but there is still a need for more studies to enhance even more the efficiency of the current drinking water treatment processes [16] or to develop new and improved technologies.

Drinking water production from seawater has an important role in reaching the United Nations Sustainable Development Goals (SDGs), and in particular the goal for clean water and sanitation (SDG 6). Considering the need to address drinking water scarcity and the increasing challenge of dealing with more frequent droughts and desertification related to climate change, the development of more and better desalination plants is a crucial step in many regions of the world, with the aim to ensure safe and affordable drinking water supply for the increasing population, without being exclusively dependent on surface freshwater and/or groundwater supply sources.

However, there is a knowledge gap on microplastics behavior and removal during desalination processes, with a search on the Scopus database on 4th of May of 2023 surprisingly giving only 9 results, when searching the article title, abstract and keywords of the documents for "desalination AND microplastics". Of those documents, some only briefly refer to desalination plants as part of the plastic pollution issue or are review articles [18–21]. Yaranal et al. reported for the first time the removal efficiency of microplastics from synthetic seawater using hollow fiber membranes during a microfiltration (MF) process, with 99.3 % success as assessed using Raman microscopy [22]. Almaiman et al. analyzed tap water sourced from desalinated seawater in Saudi Arabia, revealing low levels of contamination (<1.8 microplastics L^{-1}) when samples were analyzed by FTIR microscopy [23]. Pérez-Reverón et al. analyzed, also by FTIR microscopy, brackish water in a desalination plant in Fuerteventura (Canary Islands, Spain) that was treated by filtration with cartridges filters, dual membrane reverse osmosis and chlorination [24]. In this study, the 2.0 ± 2.0 items L^{-1} detected are hypothesized to be contaminations after the treatment and during water storage [24].

In parallel, the Scopus search for "membrane AND distillation AND microplastics" only gives 3 results, one of them available in Chinese language [25] and the others being review articles discussing membrane technologies in general: on fouling mitigation in membrane separation processes [26] or on membrane technology for sustainable water and energy management [27]. Membrane distillation is a thermally driven separation technology in which water can be extracted from the feed stream through a hydrophobic microporous membrane due to the vapor pressure gradient that is established across the membrane [28]. While there are other processes that can be used for water desalination, membrane distillation offers several benefits, such as a relatively low operating pressure, when compared to pressure-driven membrane processes like ultrafiltration or reverse osmosis, and as consequence resulting in lower equipment costs and increased process safety [29,30]. Another benefit is the water high separation efficiency, which can theoretically reach 100 % [28], removing undesired non-volatile substances, particulate matter, and microorganisms. As drawback, membrane distillation needs energy to keep the retentate at high temperature, although renewable sources of energy can be used to have a more environmentally friendly process (e.g., geothermal or solar energy). Additionally, membrane fouling, pore wetting, and mineral scaling can pose some problems depending on the feed stream [31], and the process concentrates some undesired compounds in the retentate (as other membrane processes) and does not eliminate them. However, the last disadvantage can be turned into a benefit if one or more undesired compounds with commercial value can be extracted and isolated from the retentate (e.g., mineral recovery from seawater [32], lithium from lithium-ion batteries recycling process [33], and high-added-value compounds from food industry wastewater such as protein from the meat processing waste stream [34–36]).

The research presented in this paper constitutes one of the first assessments of microplastics behavior and removal during a membrane distillation treatment, at a lab-scale. The study was aimed at analyzing i) the behavior of microplastic particles (MPPs) in a direct contact membrane distillation (DCMD) system, regarding chemical and physical modifications of the particles and their distribution and fate inside the system, and ii) the potential influence of MPPs on the DCMD process, namely on the treated water production and quality. For that, temperature stress batch experiments (using amber bottles) were first conducted with three virgin polymers: LDPE - low-density polyethylene, PET - poly(ethylene terephthalate) and uPVC - unplasticized poly(vinyl chloride). Based on the results of these experiments, uPVC was selected to test the lab-scale DCMD system at two different MPP loads and different aging degrees, in filtered seawater. The DCMD parameters, such as the vapor pressure gradient, membrane permeability for water, and the interval permeate flux, were followed during each experiment to infer the impact of the MPPs on the performance of the system. In parallel, the MPPs modifications were assessed by different characterization techniques at the end of the experiments, regarding the chemical structure, UV–visible absorption, and surface morphology. This assessment was performed since the potential degradation of the microplastics in DCMD processes can lead to a decrease of the retentate water quality and faster membrane fouling, in both cases due to the release of substances and/or smaller particles into the water. Additionally, if the retentate is released into the environment, this can contribute to the acceleration of the aging process of the microplastics in marine ecosystems by non-natural agents, with consequent implications on how they will interact with other substances and with biota in those ecosystems. Finally, the treated water was analyzed for the presence of MPPs by Raman microscopy (μRaman), assessing the removal efficiency of MPPs bigger than 1.2 μm during DCMD.

2. Material and methods

2.1. Microplastic particles (MPPs)

Virgin MPPs of LDPE (average particle diameter of 509 ± 221 μm), PET (161 ± 79 μm) and uPVC (159 ± 43 μm) were purchased in powder form from Goodfellow (UK). The main characteristics of these MPPs, regarding the physical and chemical properties and interaction with

certain organic substances, are described in our two previous articles on microplastics [37,38], which do not make use of DCMD. These three polymers were selected for this work based on i) their high share on the global plastic production: 26.9 % polyethylene (or 14.4 % specifically for LDPE and LLDPE - linear low-density polyethylene), 6.2 % PET, and 12.9 % PVC of the 390.7 Mton plastics produced in 2021 [39], and ii) because of their distinct resistance to aging stressors [37] which allows to have a better representation of the diversity of polymers that have been found in the environment [40].

2.2. Seawater (SW) and filtered seawater (FSW)

Seawater samples were collected at *Leça da Palmeira* beach, in Matosinhos, north of Portugal (Fig. A1 of the SM - Supplementary Material). The sampling site was selected since former studies with the DCMD unit at our laboratories used seawater collected there for desalination studies [41]. To ensure sample collection reproducibility, the APA/SNIRH bathing water monitorization station PTCK3P – Leça da Palmeira (EPSG:3857 coordinates: 41.190833, −8.706944) was selected [42]. The beach is characterized as an Atlantic Ocean urban beach with an extensive sand strip and rocky clusters. The potential sources of contamination at the beach include two water courses (Sardoal stream and Leça river), a wastewater treatment plant (WWTP), Leixões harbor (fishing, and cargo and passenger ships docking) and other anthropogenic activities.

US-EPA "dipping using sample container" method of surface water sampling was selected to collect the seawater samples. This method involves collecting the sample directly into the container, without disturbing the bottom sediment [43]. Bottles with a capacity of 5 L were employed for this procedure. Each open bottle was plunged straight down to a depth of 15 to 30 cm below the water surface, moved horizontally to the surface while tipped slightly to let trapped air escape, and removed in a vertical position. Approximately 2.5 cm of headspace was left in each sample container.

The seawater samples collected were preserved in cold (−18 °C) until two days before treatment in the DCMD system. Then, the samples were vacuum filtered through 47 mm glass microfiber filters (pore size 1.2 μm, purchased from VWR) to remove suspended particles (including microplastics). Due to the pore size of the filters used during vacuum filtration, environmental microplastics smaller than 1.2 μm and nanoplastics could still be present in the filtered seawater, which constitutes a limitation of this work. This pore size was selected to be closer to 1.0 μm, which is the lower size limit of microplastics according to ISO/TR 21960:2020 (that classifies nanoplastics as plastics smaller than 1 μm; however, this is not a consensual definition among the scientific community). The pH of the seawater was analyzed before (SW) and after filtration (FSW) using a Consort (Belgium) C6010 instrument: pH_{SW} = 8.27 and pH_{FSW} = 8.11 (for the samples used for the DCMD experiments).

2.3. Temperature stress (TS) batch experiments (in amber bottles)

Two sets of experiments were performed to mimic the possible plastic aging by temperature when MPPs are in suspension in the retentate during a DCMD treatment, using: i) Milli-Q ultrapure water (TS-UPW); and ii) filtered seawater (TS-FSW).

For that, 2 g of virgin MPPs of LDPE, PET or uPVC and 600 mL of ultrapure water (UPW) or filtered seawater (FSW) were added to each 1 L amber bottle, closed with aluminum foil instead of the plastic cap, thus resulting in six different experiments: LDPE/PET/uPVC TS-UPW and LDPE/PET/uPVC TS-FSW. The bottles were placed inside a paraffin bath for 24 h, which was heated continuously for the duration of the experiment to keep the ultrapure water or seawater at ca. 80 °C. The contents of the bottles and the paraffin baths were continuously stirred (850 rpm) with magnetic stirring bars with polytetrafluoroethylene (PTFE) encasement.

After 24 h, the bottles were removed from the paraffin bath and were let to cool down at room temperature. Finally, the contents of the bottles were vacuum filtered through 47 mm glass microfiber filters (pore size 1.2 μm, purchased from VWR) to separate the MPPs from the liquid phase. For that, Normax (Portugal) glass filtration kits, 1000 mL Kitasato glass flasks (LINEX, Portugal), and a VCP 80 vacuum pump (VWR) were used. The filters with the MPPs collected were stored inside soda-lime glass Petri dishes and dried in a desiccator in the dark.

The pH of the ultrapure water or filtered seawater was analyzed at t = 0 h (before adding the MPPs) and t = 24 h (after filtration) using a Consort (Belgium) C6010 instrument (Table A1 of the SM).

2.4. Direct contact membrane distillation (DCMD) system and experiments

DCMD is one of the membrane distillation (MD) configurations available [44] and the one selected for this work. In DCMD, the retentate (feed stream) and the permeate (receiving stream) are in direct contact with a porous hydrophobic membrane and both can be in recirculation. Because the retentate temperature is increased to a pre-defined high temperature and the permeate is kept at a low temperature, a vapor pressure gradient (ΔP) is created between the two sides of the membrane, being this the driving force in membrane distillation. This makes the water vapor diffuse/flow from higher to lower vapor pressure across the membrane pores and its condensation on the permeate side, leading to the production of a purified water flux from the retentate side of the membrane to the permeate side, while the particles and non-volatile undesired compounds are concentrated in the retentate side [28]. Since the membrane is hydrophobic, it prevents the penetration of the aqueous solution into the pores due to the capillary force, which results in a vapor/liquid interface at each pore entrance [29].

A laboratory-scale DCMD system was previously installed in our laboratories to conduct research related to desalination or wastewater treatment, as well as to test the performance of innovative membranes, e.g., carbon nanotubes blended membranes [45]. A LH-cell (a large cell with an H-like configuration and an effective membrane area of 70 cm^2) was selected as the membrane module for this work, based on previous work [41]. Polytetrafluoroethylene (PTFE) hydrophobic membranes with 0.22 μm pore size, 85 % porosity, liquid (water) entry pressure (LEP_W) of 280 kPa [30,46], and 150 μm thickness purchased from Merck Millipore Ltd. (reference FGLP00010) were the commercial membranes selected, based on their good performance regarding the permeate flux obtained [41]. For each experiment, a new PTFE membrane was cut and installed in the LH-cell. The lab-scale system setup, that is exclusively dedicated to desalination, is represented in Fig. 1 (the precision balance used to measure the permeate-bottle mass is not represented; see Section A1 of the SM for more information on the specific components). Both the retentate and permeate are in recirculation for the full duration of each experiment.

In order to study the behavior of MPPs in the DCMD system and test the efficiency of the treatment in their removal, five experiments were conducted:

1. **MD-PW-C** – Control experiment with purified water (PW) as feed and distilled water (DW) as receiving stream, without MPPs, during 24 h;
2. **MD-FSW-C** – Control experiment with filtered seawater (FSW) as feed, without MPPs, during 8 h;
3. **MD-FSW-TS** – 8 h experiment with FSW spiked with 0.1 g L^{-1} of TS-FSW-aged uPVC (obtained as described in Section 2.3 by aging uPVC at a given temperature in FSW);
4. **MD-FSW-V** – 8 h experiment with FSW spiked with 0.2 g L^{-1} of virgin uPVC;
5. **MD-FSW-R** – 8 h experiment with FSW spiked with 0.1 g L^{-1} of uPVC recovered (R) from the previous experiment (i.e., MD-FSW-V-aged uPVC).

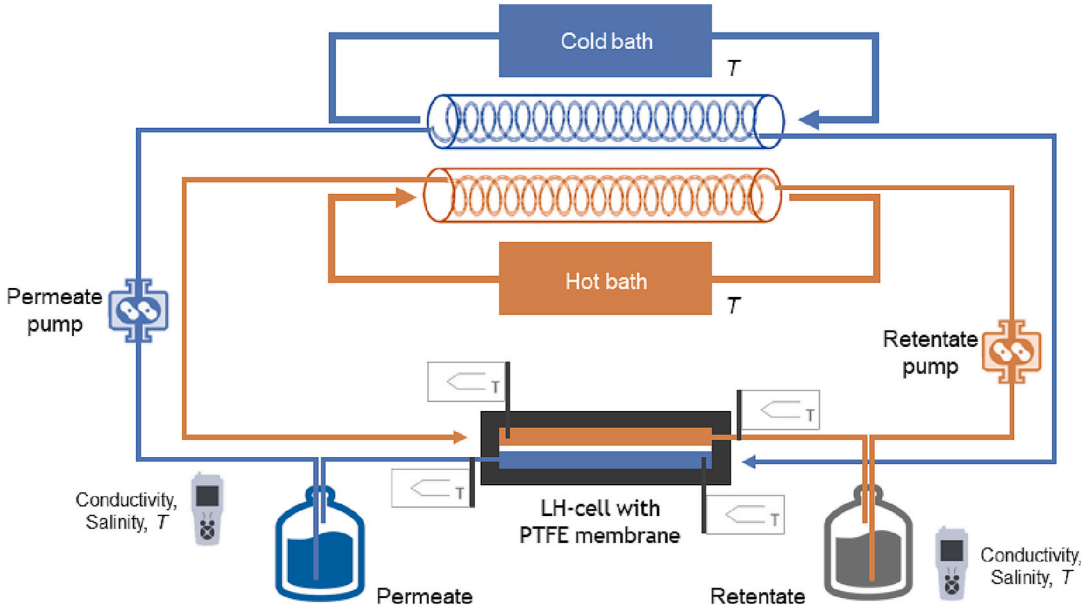

Fig. 1. Direct contact membrane distillation (DCMD) setup.

The operating parameters were set to the following values: hot bath temperature = 90 °C making the retentate being at ca. 80 °C at the LH-cell inlet; cold bath temperature = 17 °C making the permeate being at ca. 25 °C at the LH-cell inlet; peristaltic pumps flow rates = 500 mL min^{-1}. These values were defined based on short-duration experiments (at least 1 h with stable ΔP) with DW as both receiving and feed stream; these experiments were conducted previously to study the relationships between the permeate interval flux and the ΔP, or between the permeate interval flux and the retentate and permeate flow rates. The results of these experiments are included in Figs. A2 and A3 of the SM.

All the experiments followed the same main procedure (see Section A1 of the SM for more information), with the load of MPPs (0.0, 0.1 or 0.2 g L^{-1} of uPVC), sample type of uPVC (virgin, TS-FSW-aged or MD-FSW-V-aged), and feed stream (PW or FSW) being the parameters under study. Each experiment started with an initial small volume of distilled water (DW), while a volume of 10,000 mL of PW or FSW was used as feed water (see Section A1 of the SM for more information). The PW was obtained by reverse osmosis of tap water, and all the FSW used for these experiments was collected on the same day (18th October 2022). The experiment time (8 h for FSW or 24 h for PW) was selected by considering the feed initial volume (10 L) and that it was not desirable to reach a salinity concentration in the retentate that would increase the membrane mineral scaling rate and lead to flux decline. Some MD-FSW-C experiments were initially conducted for 24 h but at these conditions the high concentration of the retentate led to flux decline (started at $8 < t < 15$ h) and the contamination of the permeate quality was observed, as detected by the permeate progressively increasing conductivity after ca. 16 h of operation. Considering experimental limitations (e.g., volume of seawater feed, area of the membrane), the MD-FSW experiments time was decreased to 8 h, ensuring stable conditions after the stabilization time until the end of each experiment.

For the experiments with MPPs (MD-FSW-TS, MD-FSW-V, and MD-FSW-R), both the retentate and permeate were vacuum filtered through two 47 mm glass microfiber filters (pore size 1.2 µm, purchased from VWR) at the end of the experiment, following the same procedure as in Section 2.3. The retentate was filtered with the goal of collecting the MPPs to characterize them and identify potential modifications. The first 1 L of distilled water used to clean the retentate tubing (Section A1 of the SM) was filtered as well with the same filter, and the MPPs were washed with distilled water to remove most of the seawater salts. The permeate was filtered to enable the analysis of the presence of MPPs in the treated water. The retentate and permeate filters were weighted before filtration and after drying in the desiccator.

2.5. Characterization of the PTFE membranes

The hydrophobicity of the membrane surface was evaluated by triplicate measurements (performed in different areas of the membrane) of the purified water or seawater contact angle by an Attention Theta optical tensiometer (Biolin Scientific), using the sessile drop method and a sample volume of 3 µL. The contact angle measurements were carried out, at room temperature, on the retentate side of two dry PTFE membranes: one unused (fresh) membrane and the membrane used in the MD-FSW-V experiment (dried at room temperature). The software OneAttension was used to analyze the images recorded and perform the baseline.

Scanning Electron Microscopy (SEM) analyses were performed for the fresh and used membranes of the DCMD experiments using the Phenom ProX instrument (Thermo Fisher Scientific, USA). Additionally, the PTFE membranes were also analyzed under the WITec alpha300 R confocal Raman microscope (WITec, Germany) with the magnification of 10× with the Zeiss EC Epiplan 10×/0.25 objective. Both these analyses were performed to have a closer look at the salt crystals formed on the retentate side of the membranes and identify potential membrane fouling and mineral scaling.

2.6. Characterization of MPPs samples

The MPPs samples were characterized before and after the batch experiments used to simulate aging by temperature (Section 2.3), and before and after the DCMD experiments (Section 2.4).

ATR-FTIR measurements were completed using a FTIR-6800 spectrometer equipped with a DLaTGS detector (JASCO, Japan) with a MIRacle single reflection horizontal ATR attachment (PIKE Technologies, USA), with a ZnSe crystal. The measurements were achieved with a 4 cm^{-1} resolution of the 4000–600 cm^{-1} region, with 128 scans/sample. Background (empty and clean system) was done for every two samples analyzed. The baseline correction was performed with the Spectra Manager software, with points at 4000, 3000 (only for uPVC), 2000 and 600 cm^{-1}. In addition to the analysis of the MPPs samples with this technique, FSW salts were also analyzed. For that, FSW was left in the laboratory oven at 80 °C until all the water evaporated and the salt

crystallized.

Since uPVC MPPs changed coloration, the optical absorbance of uPVC samples was measured by UV–Visible spectroscopy using a JASCO V-560 spectrophotometer (JASCO, Japan). The baseline correction was performed with barium sulfate (Sigma-Aldrich, CAS: 7727-43-7, purity 98 %). Each measurement was performed with a 0.5 nm resolution of the 200–800 nm region.

Scanning Electron Microscopy (SEM) analyses were performed for some uPVC MPPs samples (i.e., virgin, MD-FSW-TS-aged and MD-FSW-R-aged). For that, aliquots of those samples were first coated with an Au/Pd thin film, by sputtering, using a SPI Module Sputter Coater equipment (SPI, USA). Then, the analyses were performed in low-vacuum mode, using a high-resolution (Schottky) Environmental Scanning Electron Microscope: FEI Quanta 400 FEG ESEM (FEI Company, USA).

2.7. Raman microscopy analyses

The 47 mm glass microfiber filters (pore size 1.2 μm, purchased from VWR), used to vacuum filtrate the permeate after the MPPs experiments with the DCMD system, were analyzed for the presence of MPPs. No pre-treatment step (density separation or digestion) of the water samples was performed since low levels of particles or organic matter were anticipated for the treated water. Raman microscopy (μRaman) measurements were made using a WITec alpha300 R confocal Raman microscope (WITec, Germany) that uses a WITec UHTS 300 VIS spectrometer (600 lines/mm grating) coupled with a FI CCD detector (spectral resolution of 0.8 cm^{-1}/pixel, 1650 × 200 pixels, −60 °C).

Two randomly selected areas per filter (one at the center and the other at the edge of the filter) were selected at a magnification of 50×. Then, the spectra were recorded using 10 mW of laser power and the 532 nm excitation wavelength, with 5 accumulations and an integration time of 1 s per spectrum. An aliquot of virgin uPVC and one unused filter were analyzed to add those spectra to the system library as reference. The data processing was achieved with the Project FIVE and WITec ParticleScout software.

2.8. Data analysis

Detailed information on the calculations performed with the DCMD data can be found in section A2 of the SM. In summary, the vapor pressure gradient (ΔP) for each data point was estimated using the equation for the ΔP for counter-current flow (Eq. A1). For that, the partial vapor pressures at the inlet and outlet temperatures of the permeate and retentate side of the membrane cell were calculated by applying the Antoine equation (Eq. A2). The interval permeate flux (J) was calculated for each data point based on the measurements of the distillate produced in each time interval, and on the known effective area of the membrane (Eq. A4). Based on the calculated ΔP and J, the membrane permeability for water (B) can be estimated since it corresponds to the slope of the linear regression of J as function of ΔP (Eq. A3). The measured uncompensated conductivity was converted to the compensated conductivity (EC_{25}) based on the temperature compensation factor and the measured temperature (Eq. A5). The water recovery (%) was calculated as the percentage of distilled water produced from the water feed, while the rejection parameter (%) expresses the membrane impermeability for the seawater salts based on the salinity measurements.

Whenever possible, the average and respective standard deviation were calculated for the experimental data. The graphical representation of the results and model fitting were performed with the OriginPro 9 software, while Microsoft Excel was used to obtain the above-mentioned calculations.

3. Results and discussion

The temperature stress (TS) batch experiments with MPPs in amber bottles, carried out before the DCMD experiments, allowed to study the individual effect of exposing the MPPs to a temperature stress when in suspension in water. As explored in Sections 3.1 and 3.2, thermal degradation and, to a lesser degree, hydrolysis are probably the main aging mechanisms at play, since there were very few signs of oxidation due to the absent or very low increase of oxygen-containing functional groups on the MPPs, and taking into account the type of experiments performed. Based on the results of those experiments with three polymers, uPVC was selected to study the behavior of MPPs in a lab-scale DCMD system, which is explored in Section 3.2 (potential MPP aging, and their mobility and fate in the system), Section 3.3 (impact in the DCMD system performance) and Section 3.4 (DCMD performance in keeping MPPs from the permeate).

3.1. LDPE and PET under temperature stress (in amber bottles)

Very fast fouling of the membranes was observed during the vacuum-filtration of the LDPE samples, particularly for the LDPE MPPs aged at ca. 80 °C in filtered seawater (TS-FSW-aged samples). A film was deposited on the filter (Fig. A4a of the SM), consisting mainly of seawater salts (primarily NaCl; major ion composition of the FSW was analyzed by ion chromatography and included in Table A2 of the SM) and LDPE, according to the ATR-FTIR analysis for the TS-FSW-aged sample (Fig. A5 of the SM), which might be the cause for the filter fouling. For the LDPE MPPs aged at ca. 80 °C in ultrapure water (TS-UPW-aged samples), a minor change in the electric conductivity of the water sample was detected, increasing from 5.3 μS cm^{-1} to 12.8 μS cm^{-1}, which was a higher increase than what was observed for PET (8.0 μS cm^{-1}) and uPVC (6.9 μS cm^{-1}), even if these values are very low. The electric conductivity of UPW solutions spiked with each polymer, under the same load as the TS experiments but measured at room temperature (ca. 24 °C) after 24 h, resulted in increases of ≤2 μS cm^{-1} before filtration (from 5.3 μS cm^{-1} for UPW to 6.0 μS cm^{-1} after 24 h with LDPE, and to 8.0 μS cm^{-1} after its filtration). The combination of these two results (formation of a film on the TS-FSW filter and slightly increase in the conductivity of TS-UPW solution) suggests the release of some substances from LDPE MPPs to the water due to the degradation of the polymer. However, these conductivity values are quite low and further studies would be necessary to confirm this hypothesis.

The ATR-FTIR spectra of the LDPE samples (Fig. A5 of the SM) show very few modifications of the LDPE chemical structure, with most of the new absorption bands resulting from interference of the FSW salts (which were also analyzed by ATR-FTIR; FSW salts spectrum included in Fig. A5 of the SM). Indeed, the LDPE TS-UPW-aged sample only has some minor modifications with a very small increase of the C═O absorption at 1717 cm^{-1} (carbonyl species), and distortion of the LDPE medium intensity characteristic absorption peaks at 1468 cm^{-1} (CH_2 bending deformation) and at 718 cm^{-1} (CH_2 rocking deformation). The LDPE TS-FSW-aged sample has the same modifications identified for the LDPE TS-UPW-aged sample, with the additional increase of the absorption intensity at the bands 3712–2987 cm^{-1}, 1155–920 cm^{-1} and 700–600 cm^{-1}, which can be related to the presence of FSW salts.

From visual observation of the PET samples, no signs of polymer degradation were identified, although salt crystals were observed mixed with the PET MPPs on the TS-FSW-aged sample (Fig. A4b of the SM). The ATR-FTIR analysis (Fig. A6 of the SM) did not allow to identify any modification in the chemical structure of the polymer for the TS-UPW-aged sample. For the TS-FSW-aged sample, there was an increase in the absorption intensity at 3761–2980 cm^{-1} band, the band near 972 cm^{-1} (O—CH_2 stretching of ethylene glycol segment in PET) [47,48] and the 700–600 cm^{-1} band. While these can be interferences from the FSW salts (Fig. A5 of the SM), the band near 972 cm^{-1} has been used before by Cobbs and Burton [49] to follow the crystallization of PET on heating, since it is one of the crystallinity-sensitive bands of that polymer [50].

3.2. uPVC under temperature stress (in amber bottles) and behavior in a lab-scale DCMD system

Visual observation of the uPVC samples revealed that after the temperature stress batch experiments, both the TS-UPW-aged and TS-FSW-aged samples acquired a pinkish coloration (Fig. A4c of the SM). This change in coloration was analyzed in more detail by UV–Visible spectroscopy. The results (Fig. 2) of the two aged samples show increased absorption for visible wavelengths (380–750 nm), with maximum absorption at 443 nm. The lower absorption of these samples in the red region (620–750 nm) of the visible spectrum results in a higher emission in that wavelength, giving the samples their pinkish coloration. These results are in agreement with what was previously observed by De Campos and Martins Franchetti [51] after thermally treating PVC (1 h at 130 °C). This discoloration of PVC has been previously described in the literature as *pinking*, with short chain conjugated polyenes being identified as the most likely functional groups responsible for the development of the pink color [52–55]. In the present study, the *pinking* was the result of thermal degradation of the surface of the MPPs in conditions of reduced light and high moisture, and under temperatures of ca. 80 °C, being observed for the TS-UPW-aged, TS-FSW-aged, and MD-FSW-TS-aged samples of uPVC. It should be noted that while the temperature of the retentate reached values of ca. 80 °C at the entrance of the LH-cell during the DCMD experiments (listed in Table A3 of the SM), most of the volume stayed at lower average (after 4 h) temperatures inside the retentate container (as recorded by the conductivity meter): MD-PW-C (24 h) = 69.1 ± 0.3 °C, MD-PW-C (first 6.5 h) = 69.2 ± 0.1 °C, MD-FSW-C = 70.2 ± 0.2 °C, MD-FSW-V = 70.7 ± 0.1 °C, MD-FSW-*R* = 70.2 ± 0.2 °C, MD-FSW-TS = 69.8 ± 0.4 °C.

For both TS-aged samples, there was increased absorption in the UV region of the spectrum (Fig. 2); however, much more distinctly with the TS-FSW-aged sample. The most substantial difference between the two samples was detected for 250–300 nm, due to the increase of the absorption of short-wave UV (UV-C) and middle-wave UV (UV-B). This suggests that this increase in the absorption in the UV region is mostly due to the seawater constituents.

ATR-FTIR measurements were performed for uPVC samples after the temperature stress batch experiments but also after the DCMD treatments. This polymer was selected for the experiments in the lab-scale DCMD system since the temperature stress batch experiments showed that thermal degradation occurred for uPVC but, contrary to what was observed for LDPE, there was a lesser risk of membrane fouling due to the polymer degradation. The ATR-FTIR results (Fig. 3) show the increase of the absorption intensity at the 3750–2988 cm^{-1} band for the TS-FSW-aged sample, after the DCMD treatment with the TS-FSW-aged sample (MD-FSW-TS-aged) and after two DCMD treatments of the virgin uPVC (MD-FSW-R-aged). Since the TS-FSW-aged sample was not rinsed with distilled water, while the DCMD samples were rinsed, and the band intensity is much higher for the TS-FSW-aged sample and decreased for the same sample after the DCMD treatment (MD-FSW-TS, Fig. 3), this suggests that the increase at this band is mostly due to the presence of FSW salts. Similarly, there was increased absorption at the 1094–958 cm^{-1} band for the MD-FSW-TS-aged sample, and particularly for the TS-FSW-aged sample. This is expected to be another FSW salts interference.

The increased absorption at 1645 cm^{-1} observed for the TS-FSW-aged uPVC sample is expected to be the interference of the FSW salts, since their analysis revealed an absorption band with a maximum at 1638 cm^{-1} (included in Fig. A5 of the SM). However, for the MD-FSW-TS-aged and MD-FSW-R-aged samples there was increased absorption for the 1718–1450 cm^{-1} band, with a maximum at 1600 cm^{-1}. The increased absorption in this region can be due to the formation of conjugated polyenes sequences (—CH═CH) in the polymer chains, suggesting that the DCMD treatment was effective in modifying the chemical structure of uPVC in those two experiments. No modifications of the chemical structure were identified for TS-UPW-aged and MD-FSW-V-aged uPVC samples. Therefore, no correlation between the

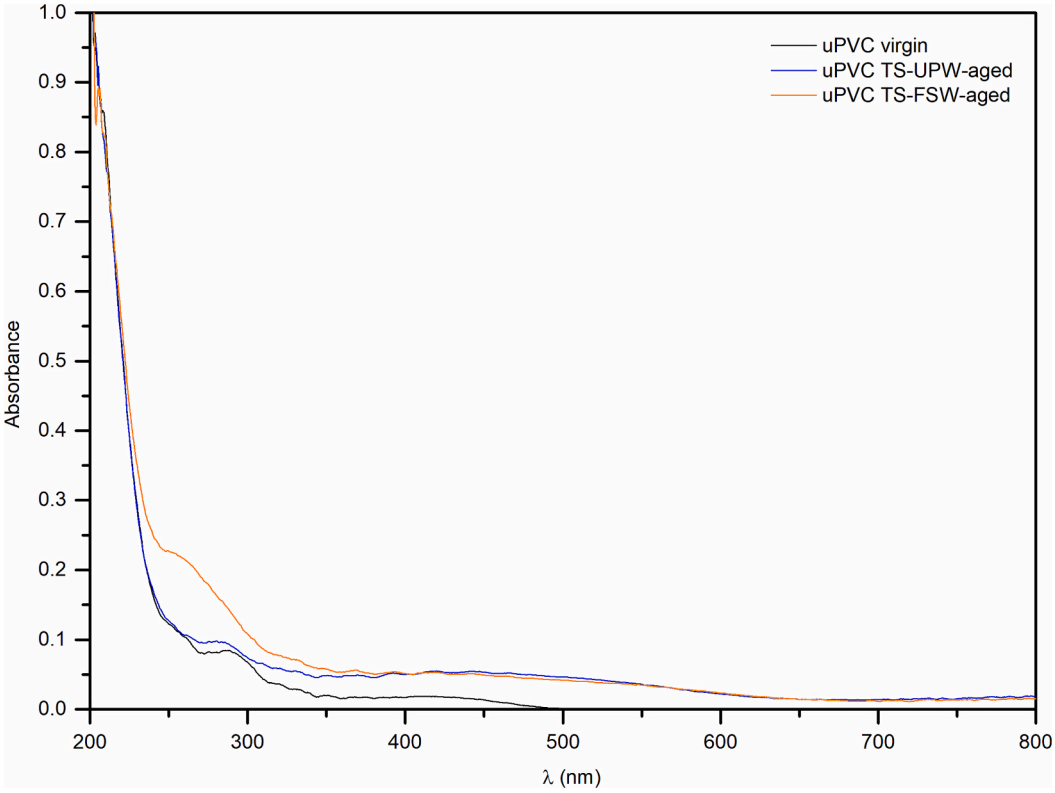

Fig. 2. UV-VIS spectra for unplasticized poly(vinyl chloride) (uPVC) before and after the temperature stress (TS) batch experiments (t = 24 h; T = 78–82 °C; V = 600 mL of UPW or FSW with 2 g of virgin uPVC).

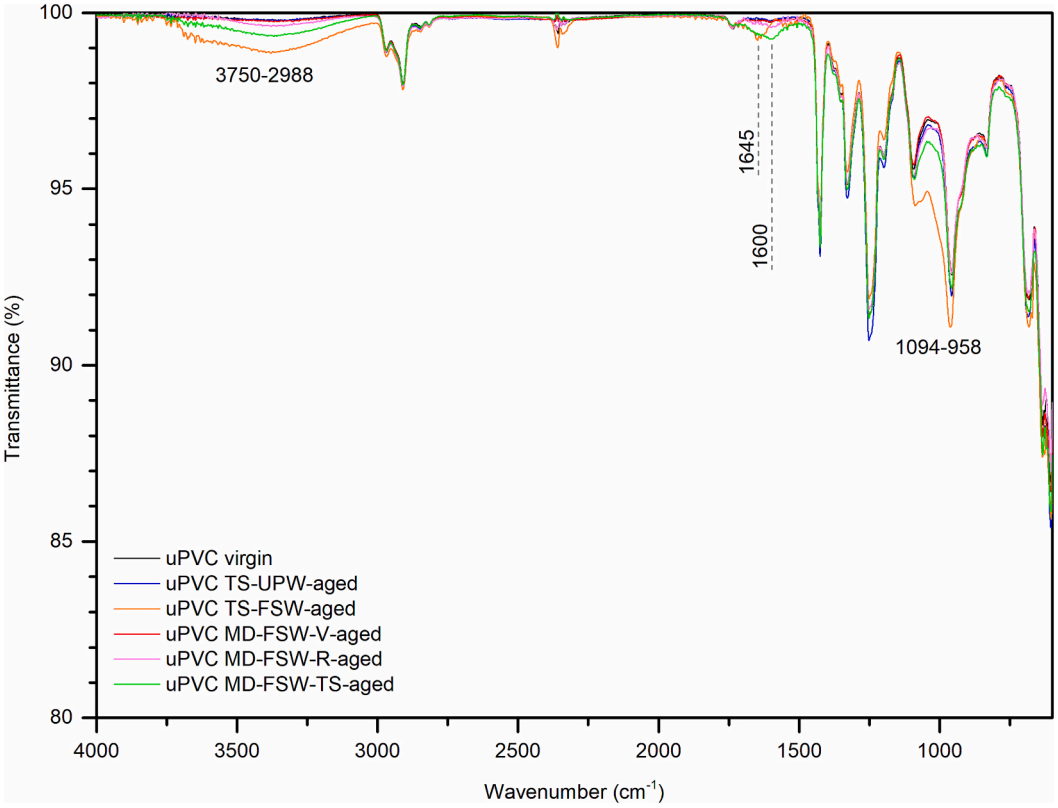

Fig. 3. ATR-FTIR spectra for unplasticized poly(vinyl chloride) (uPVC) before and after the temperature stress (TS) batch experiments (t = 24 h; T = 78–82 °C; V = 600 mL of UPW or FSW with 2 g of virgin uPVC) and the DCMD experiments (V_{feed} = 10 L of FSW spiked with MPPs; Q = 500 mL min^{-1}; under stable conditions: $T_{P,IN}$ = 23–24 °C and $T_{R,IN}$ = 79 °C).

pinking of the TS-UPW-aged, TS-FSW-aged and MD-FSW-TS-aged samples (Fig. A4c of the SM) and the polyene group (MD-FSW-TS-aged and MD-FSW-R-aged samples) could be reached. This lack of correlation can be due to a different ratio/amount of formed and oxidized polyenes during the experiments and their lengths [56] since the TS and DCMD experiments were conducted under different light and dissolved oxygen conditions.

The SEM analysis of uPVC samples after the MD-FSW-TS and MD-FSW-R treatments did not allow to identify any relevant surface, shape, or size modification in comparison with the virgin uPVC (Fig. A7 of the SM). This was expected considering that no modification was detected for uPVC after more aggressive treatments that were conducted previously by the research group [37], and the observed surface heterogeneity of the uPVC particles acquired. The surface morphology of the uPVC MPPs used for this study is composed of two main morphologies (Fig. A8 of the SM): i) areas with irregular but smoother surfaces, and ii) areas with more uniform but very rough surfaces (granular). In both areas, small pores can be observed (Fig. A7 of the SM).

Regarding the physical behavior (i.e., mobility and fate) of the uPVC MPPs during the DCMD treatments, the presence of MPPs was detected inside the LH-cell, on the retentate side (Fig. A9a of the SM). In addition, the procedure used to clean the retentate tubing at the end of each experiment (described in Section A1 of the SM and Section 2.4), allowed to recover uPVC MPPs that remained in the retentate circuit until that step. This confirms that at least some MPPs were able to recirculate with the retentate in the DCMD system. However, since the retentate container was not agitated, most of the MPPs stayed sedimented on the bottom of the retentate container and only a portion in suspension (Fig. A9b of the SM). This constitutes one of the limitations of these experiments conducted with MPPs, because the MPP mechanical aging was reduced (main mechanism of degradation was the thermal stress), and because the potential impact on the DCMD system operation was also reduced.

3.3. Influence of uPVC MPPs on the DCMD process

The MD-PW-C experiment was carried out for 24 h with the main goal of testing the system with the combination of operating parameters and volume of feed selected for this study (Section 2.4), while also enabling the estimation of the maximum distilled water production under those conditions.

The MD-PW-C stable conditions were reached after ca. 3 h of operation and no flux decline was observed (Fig. 4). The system stabilization time results mainly from the feed (purified water for the MD-PW-C experiment or filtered seawater for the MD-FSW experiments) being at room temperature inside the container at t = 0 h, making the stabilization time being dependent on the volume used as higher volumes take more time to heat. An average ΔP of 35.7 ± 0.4 kPa and permeate interval flux of 38.9 ± 0.3 kg m^{-2} h^{-1} were maintained for t = 4–6.5 h and t = 15.5–24 h of operation, corresponding to a membrane permeability for water of 1.09 ± 0.02 kg m^{-2} h^{-1} kPa^{-1}. Based on the difference between the measurement of the total volume of permeate produced and the volume of permeate produced during the data collection, the volume produced during the night was estimated and, from that, resulted the estimated average permeate interval flux of 39.1 kg m^{-2} h^{-1} for the night period (t = 6.5–15.5 h). These results (t = 4–24 h) are aligned with the results obtained under the same operating conditions when studying the system operating parameters with DW (Figs. A2 and A3 of the SM; stable ΔP = 34.7 ± 0.2 kPa, stable J = 39.1 ± 0.4 kg m^{-2} h^{-1}). Moreover, the water recovery reached 65 % at t = 24 h, with no signs of membrane fouling and a good permeate water quality (Tables A4 and A5 of the SM).

The previous experiment with PW was carried out for 24 h, while those that followed with FSW as feed were carried out for only 8 h, as

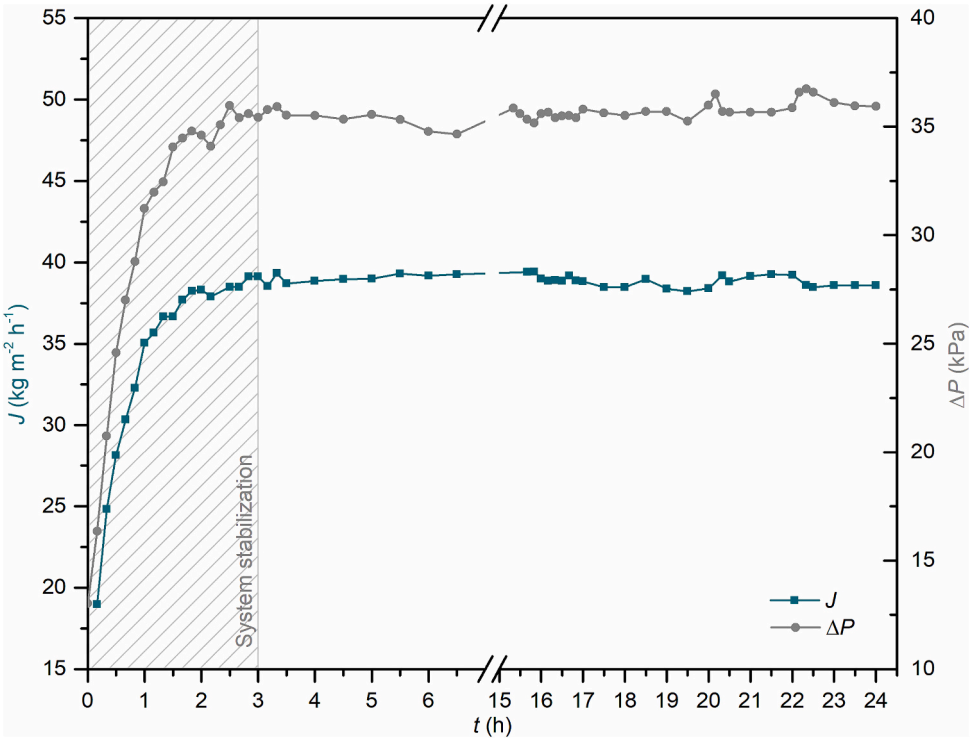

Fig. 4. Vapor pressure gradient and permeate interval flux through time for the MD-PW-C 24 h experiment (V_{feed} = 10 L of PW; Q = 500 mL min^{-1}; under stable conditions: $T_{P,IN}$ = 25 °C and $T_{R,IN}$ = 79 °C).

further explained in Section 2.4. A total of four experiments (MD-FSW) were conducted with seawater to study potential changes in the performance of the DCMD system when MPPs are in suspension in seawater. As represented in Fig. 5, the control experiment with FSW (MD-FSW-C) and the two experiments with 0.1 g L^{-1} of MPPs (MD-FSW-R and MD-FSW-TS) have the same stable ΔP (ca. 37 kPa), while the experiment

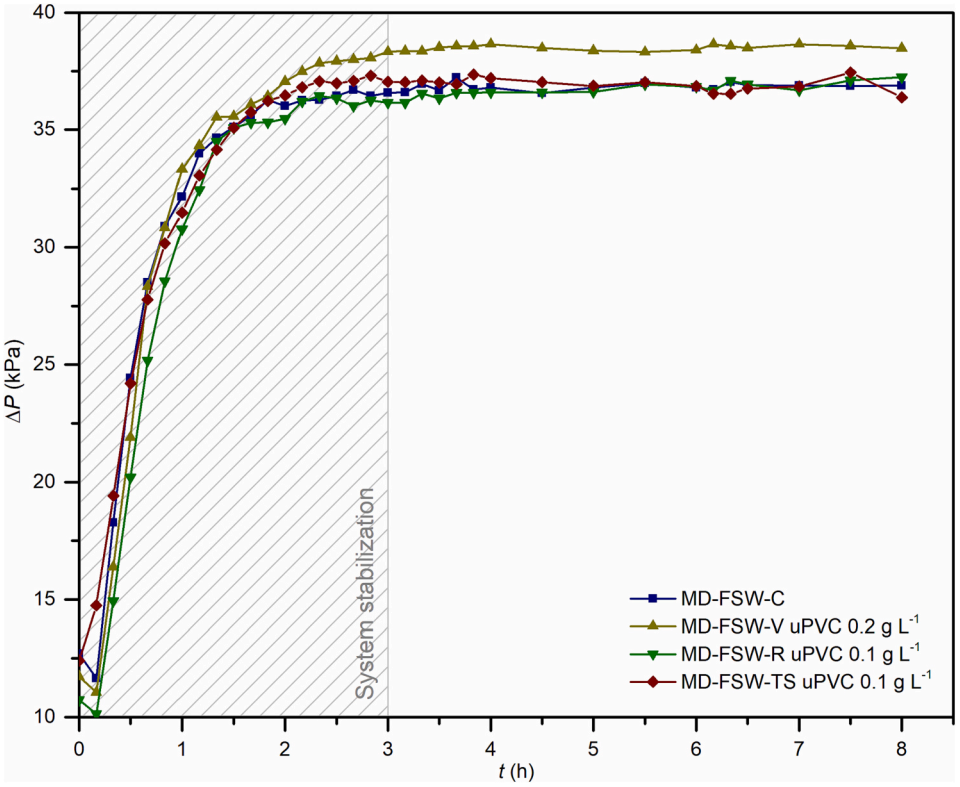

Fig. 5. Vapor pressure gradient through time for the 8 h MD-FSW experiments (V_{feed} = 10 L of FSW; Q = 500 mL min^{-1}; under stable conditions: $T_{P,IN}$ = 23–24 °C and $T_{R,IN}$ = 79 °C).

with the higher MPP load of 0.2 g L^{-1} (MD-FSW-V) achieved a higher stable ΔP of 38.5 ± 0.1 kPa. This could have happened due to slight variations in the heat transfer (e.g., in the heat exchangers) and/or in the heat losses during the MD-FSW-V experiment (e.g., less heat losses in the retentate circuit or container) compared to the other three (Table A3 of the SM). Still, since uPVC has a smaller specific heat capacity (1000–1500 J K^{-1} kg^{-1}, according to the supplier) than FSW, the specific heat capacity of the mixture is lower than that of FSW, leading to less energy being needed to change the temperature of the mixture. However, the first hypothesis is more likely since the mass of MPPs (1 or 2 g) is negligible in the FSW-MPPs mixture. Nevertheless, it was observed that DCMD experiments with FSW consistently reached higher ΔP than those of DW or PW, which could also be explained by the lower specific heat capacity of FSW when compared with DW/PW.

As expected, the stable permeate interval flux results of the four experiments (Fig. 6) are below the one obtained for the MD-PW-C experiment (Fig. 4). The following trend was observed: MD-PW-C > MD-FSW-C > MD-FSW-TS ≥ MD-FSW-R > MD-FSW-V. Therefore, these results suggest that the presence of MPPs in suspension might influence the membrane permeability for water and, consequently, the permeate interval flux, with higher MPP loads decreasing the flux (Table A4 of the SM). This is particularly evident for the experiment with the highest MPP load (MD-FSW-V), since it is the one with the highest stable ΔP and lowest stable J, leading to the lowest stable B of 0.75 ± 0.01 kg m^{-2} h^{-1} kPa^{-1}. As a result, that is also the experiment with the lowest water recovery (Table A4 of the SM), with none of the experiments showing signs of flux decline. Under the conditions studied, the uPVC MPP aging degree (MD-FSW-R and MD-FSW-TS experiments) played a less important role than the MPP load on the permeate flux.

As listed in Table A5 of the SM, all experiments produced a permeate with good water quality concerning conductivity (maximum 10.6 μS cm^{-1}) and salinity (0.0 ppt). Therefore, there are no signs of contamination of the permeate or decrease in the salt rejection efficiency. It should be noted that a disinfection step (e.g., UV) would be advisable to ensure that the water produced fulfills all requirements regarding the microbiologic parameters as set by the EU Drinking Water Directive [57].

Membrane fouling was minor (A14a and Fig. A14b of the SM for membrane cross-sections) and did not affect the permeate flux through time. The surfaces of both PTFE and PVC are expected to be negatively charged [58–60] in FSW (pH = 8.11), which limits the interaction between the PTFE membrane and the uPVC MPPs or the FSW anions, due to electrostatic repulsion. In all MD-FSW type experiments, it was similarly detected the presence of salt crystals on the membrane retentate side (Figs. A10, A11 and A12 of the SM), with mineral scaling affecting more the border of the membrane (Fig. A13 of the SM; extent of 1.0 to 1.5 cm around the membrane limit) than the center (Fig. A14c to f of the SM, showing the membrane ca. 2.0 cm from the membrane limit). The SEM images obtained (Figs. A13 and A14 of the SM) did not show a clear different pattern between the four MD-FSW membranes (including the control without MPPs), with the salt crystals populating the same areas of the membrane and presenting very diverse morphologies and sizes (see Table A2 of the SM for the major ion composition of the FSW). It should be noted that the vacuum filtration pre-treatment of the SW samples decreased the fouling of the membranes significantly, since the suspended solids (e.g., sediment) were removed. The PW or FSW contact angle measurements revealed higher contact angles for PW and the new membrane than FSW and the MD-FSW-V used membrane: PW_{new} = 142.7° ± 1.7° (in agreement with previous works [41]), PW_{MD} = 127.5° ± 5.8°, FSW_{new} = 133.4° ± 2.0°, and FSW_{MD} = 114.4° ± 4.6°. Considering only the NaCl concentration, it would be predicted that the FSW contact angle would be higher than the PW one for the same membrane, due to its higher water surface tension [61]. However, this was not observed here and can be the result of other substances dissolved in the FSW since it is an environmental sample. As expected [62,63], the contact angle of the virgin membrane (when in contact with PW or FSW)

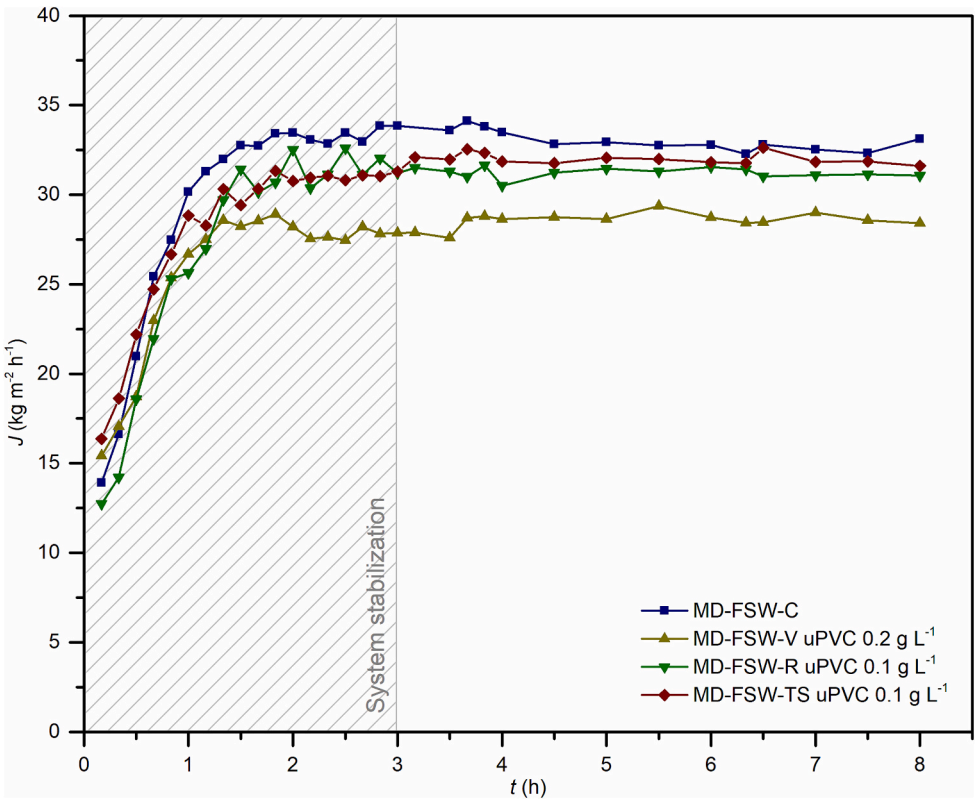

Fig. 6. Permeate interval flux through time for the 8 h MD-FSW experiments (V_{feed} = 10 L of FSW; Q = 500 mL min^{-1}; under stable conditions: $T_{P,IN}$ = 23–24 °C and $T_{R,IN}$ = 79 °C).

was higher than that of the used membrane since, as previously mentioned, the used membranes showed salt crystals on their surfaces, increasing the affinity between the liquid and the surface. While a 14.2 % reduction in the seawater contact angle was observed after the experiment, the hydrophobicity of the membrane was not compromised. Although the present work did not explore membrane reuse, every evidence points to that possibility, particularly if the membrane is cleaned [41].

3.4. DCMD performance in removing uPVC MPPs

Although the primary goal of this work was not to test the efficiency of the DCMD system in keeping the MPPs from the permeate, the treated water produced in each of the three experiments with MPPs was vacuum filtrated and the filters were analyzed for the presence of MPPs by μRaman. Before that, an unused glass filter and a sample of virgin uPVC were analyzed to be used as reference (Fig. A15 of the SM).

Almost all the particles quantified using the WITec ParticleScout (Table A6 and Fig. A16 of the SM) were identified as irregularities of the glass filter or as fluorescent impurities. Still, the Raman spectrum of one particle in each filter indicated the presence of other particles in the treated water. Of those three particles (Fig. A17 of the SM), only the one in the MD-FSW-V filter could potentially be identified as uPVC. That particle is purple and has a 2.2 μm length, 1.7 μm width and a circularity of 0.811. Therefore, it is highly unlikely that this particle is one of the uPVC added MPPs and most probably is a contamination. The particle in the MD-FSW-R filter has a length of 7.0 μm and a width of 0.7 μm, suggesting that it is a fiber. The biggest unidentified particle was on MD-FSW-TS filter and has a 46.6 μm length and 34.2 μm width, with no match to the reference spectra of uPVC. The most probable cause of these contaminations is the incorporation of air impurities by the permeate in the uncapped container used with the precision scale during DCMD, which is also a possible explanation for the slight increase in the conductivity of the permeate (Table A5 of the SM). In light of these observations, it is recommended that future research should include the pre-treatment of the permeate, with a digestion step, to remove organic matter and have a faster analysis of each filter. Similarly, the glass fiber filters used should be substituted by others with smoother surfaces.

The mass of the dried filters, used to vacuum filtrate the treated water, was practically unchanged ($\Delta m \leq 0.0003 \pm 0.0001$ g). The mass of MPPs recovered from the experiments was higher than 99.3 %, as assessed by weighting the filters used to vacuum filtrate the retentate. Taking this into account and the lack of evidence of the spiked MPPs on the treated water filters, the DCMD system has a very high efficiency (≥99 %) in removing MPPs bigger than 1.2 μm from water. This result was expected and is in line with what has been observed when membrane technologies are used to remove MPPs from water [22].

4. Conclusions

The research presented allowed to study the behavior and influence of MPPs in a lab-scale DCMD system, while being used for a desalination process. Therefore, this study constitutes one of the first on this specific topic, namely regarding the analysis of MPPs for DCMD applications.

Concerning the behavior of the MPPs in a DCMD system, due to the relatively high temperatures that the retentate can reach, the treatment can potentially lead to the degradation of the polymers and the release of substances and/or smaller particles into the water. This can be problematic since the quality of the retentate water is further decreased during the treatment, whereas membrane fouling (and consequently flux decline) can occur faster. Of the three polymers studied, only LDPE results from the temperature stress test suggest that this polymer could potentially create this problem. However, other more temperature-sensitive polymers, such as temperature-responsive polymers, could pose some additional challenges to a desalination process using a DCMD system. In parallel, PET showed very slight modifications after the temperature stress treatment and uPVC MPPs underwent *pinking*. These results led to the selection of uPVC to conduct the studies with the DCMD system.

The majority of uPVC MPPs sedimented in the retentate container since it was not agitated. Still, MPPs were found at the LH-cell (retentate side) at the end of the experiment, suggesting that, even at this lab-scale, MPPs can be in recirculation in a DCMD system. Nevertheless, this limited the MPP mechanical aging, with thermal degradation and hydrolysis being hypothesized to be the main degradation mechanisms that could increase the aging degree of MPPs during these experiments. Since minor modifications were identified for a longer period than what is expected for a desalination treatment (uPVC MPPs showed very few modifications of the chemical structure and no modifications of the surface morphology), it is anticipated that the aging of MPPs can be negligible, although it could increase significantly based on lower resistance of the polymers to higher temperatures. Further studies would be necessary to investigate the behavior of polymers with lower densities and that would more easily stay in suspension, and likewise the more temperature-sensitive polymers. Moreover, it could be tested: i) if the degradation of polymers aged during DCMD could increase their posterior degradation by other abiotic or biotic mechanisms (e.g., rate of degradation of biodegradable polymers after going through a DCMD treatment), and ii) the potential release of volatile substances by MPPs with additives, which could transfer across the membrane and contaminate the permeate, compromising the DCMD use for drinking water production.

Regarding the potential influence of MPPs on the DCMD process, the results indicate that higher MPP loads (>0.1 g L^{-1}) might have some influence on the membrane permeability for water and, consequently, the permeate interval flux and water recovery. However, the tested MPP loads are much higher than those usually found in the environment. Even so, the quality of the water produced has not decreased in any studied scenario with MPPs. Therefore, the presence of MPPs that are relatively resistant to temperature is expected to have minimal interference with the normal working of a desalination unit based on a DCMD system. As future research on this topic, the investigation of the amount of MPPs that reaches the membrane and recirculates in the system (agitated versus not agitated container) could provide useful information on the interaction between the MPPs and the PTFE membrane, and on how the presence of MPPs can interfere with the permeate interval flux.

Finally, no signs were found of the added uPVC MPPs in the treated water produced (permeate), as assessed by μRaman. All the results suggest a very high efficiency (≥99 %) in removing MPPs from water when using a DCMD system. Thus, DCMD is an alternative to other technologies, such as reverse osmosis, to obtain MPPs-free drinking water from seawater. Further studies would be necessary to study the removal efficiency for plastic particles smaller than 1.2 μm (pore size of the vacuum filters used) and particularly for nanoplastics removal assessment (DCMD membrane used with 0.22 μm pore size). Since the retentate is going to have a higher load of MPPs compared to the raw seawater, it is advised that the retentate is treated before being returned to the sea.

CRediT authorship contribution statement

Mariana N. Miranda: Conceptualization, Methodology, Investigation, Formal analysis, Visualization, Writing – original draft. **A. Rita T. Fernandes:** Methodology, Investigation, Writing – review & editing. **Adrián M.T. Silva:** Supervision, Methodology, Resources, Writing – review & editing. **M. Fernando R. Pereira:** Supervision, Conceptualization, Funding acquisition, Writing – review & editing.

Declaration of competing interest

The authors declare that they have no known competing financial

interests or personal relationships that could have appeared to influence the work reported in this paper.

Data availability

Data will be made available on request.

Acknowledgments

This work was financially supported by: LA/P/0045/2020 (ALiCE), UIDB/50020/2020 and UIDP/50020/2020 (LSRE-LCM), funded by national funds through FCT/MCTES (PIDDAC). M.N.M. and A.R.T.F. acknowledge the PhD research grants from Fundação para a Ciência e a Tecnologia (FCT) (Ref. PD/BD/137730/2018, COVID/BD/152633/2022, and 2022.12141.BD), funded by national funds and by the European Union (EU) through the European Social Fund (ESF). Scientific collaboration established under project NORTE-01-0145-FEDER-000069 (Healthy Waters), supported by North Portugal Regional Operational Program (NORTE 2020), under the PORTUGAL 2020 Partnership Agreement, through the European Regional Development Fund (ERDF). The authors are grateful to Daniela Silva and CEMUP (Portugal) for technical assistance and advice with SEM analyses of the microplastic particles, to Yaidelin A. Manrique (LSRE-LCM) for the SEM analyses of the PTFE membranes, and to Luís Carlos Matos (FEUP) for the technical assistance in the Raman microscopy measurements. The authors also acknowledge the anonymous reviewers for critical reading and whose suggestions helped improve and clarify this article.

Appendix A. Supplementary data

Supplementary data to this article can be found online at https://doi.org/10.1016/j.desal.2023.116846.

References

[1] S. Sharma, B. Sharma, S. Dey Sadhu, Microplastic profusion in food and drinking water: are microplastics becoming a macroproblem? Environ Sci Process Impacts 24 (2022) 992–1009, https://doi.org/10.1039/D1EM00553G.
[2] World Health Organization, Dietary and Inhalation Exposure to Nano- and Microplastic Particles and Potential Implications for Human Health, Geneva, https://www.who.int/publications/i/item/9789240054608, 2022.
[3] E. Garrido Gamarro, V. Costanzo, Microplastics in Food Commodities - A Food Safety Review on Human Exposure through Dietary Sources, FAO, Rome, 2022, https://doi.org/10.4060/cc2392en.
[4] A. Al Mamun, T.A.E. Prasetya, I.R. Dewi, M. Ahmad, Microplastics in human food chains: food becoming a threat to health safety, Sci. Total Environ. 858 (2023), 159834, https://doi.org/10.1016/j.scitotenv.2022.159834.
[5] M.B. Paul, V. Stock, J. Cara-Carmona, E. Lisicki, S. Shopova, V. Fessard, A. Braeuning, H. Sieg, L. Böhmert, Micro- and nanoplastics – current state of knowledge with the focus on oral uptake and toxicity, Nanoscale Adv. 2 (2020) 4350–4367, https://doi.org/10.1039/D0NA00539H.
[6] M. Sewwandi, H. Wijesekara, A.U. Rajapaksha, S. Soysa, M. Vithanage, Microplastics and plastics-associated contaminants in food and beverages; global trends, concentrations, and human exposure, Environ. Pollut. 317 (2023), 120747, https://doi.org/10.1016/j.envpol.2022.120747.
[7] J.C. Prata, J.L. Castro, J.P. da Costa, M. Cerqueira, A.C. Duarte, T. Rocha-Santos, Airborne Microplastics, in: Handb. Microplastics Environ., Springer International Publishing, Cham, 2020, pp. 1–25, https://doi.org/10.1007/978-3-030-10618-8_37-1.
[8] N.S. Soltani, M.P. Taylor, S.P. Wilson, International quantification of microplastics in indoor dust: prevalence, exposure and risk assessment, Environ. Pollut. 312 (2022), 119957, https://doi.org/10.1016/j.envpol.2022.119957.
[9] H.A. Leslie, M.J.M. van Velzen, S.H. Brandsma, A.D. Vethaak, J.J. Garcia-Vallejo, M.H. Lamoree, Discovery and quantification of plastic particle pollution in human blood, Environ. Int. 163 (2022), 107199, https://doi.org/10.1016/j.envint.2022.107199.
[10] A. Ragusa, V. Notarstefano, A. Svelato, A. Belloni, G. Gioacchini, C. Blondeel, E. Zucchelli, C. De Luca, S. D'Avino, A. Gulotta, O. Carnevali, E. Giorgini, Raman microspectroscopy detection and characterisation of microplastics in human breastmilk, Polymers (Basel). 14 (2022) 2700, https://doi.org/10.3390/polym14132700.
[11] G. Kutralam-Muniasamy, V.C. Shruti, F. Pérez-Guevara, P.D. Roy, Microplastic diagnostics in humans: "the 3Ps" progress, problems, and prospects, Sci. Total Environ. 856 (2023), 159164, https://doi.org/10.1016/j.scitotenv.2022.159164.
[12] X. Yang, Y.B. Man, M.H. Wong, R.B. Owen, K.L. Chow, Environmental health impacts of microplastics exposure on structural organization levels in the human body, Sci. Total Environ. 825 (2022), 154025, https://doi.org/10.1016/j.scitotenv.2022.154025.
[13] World Health Organization, Microplastics in Drinking-water, Geneva, 2019, https://doi.org/10.1192/bjp.112.483.211-a.
[14] A. Mohammadi, S. Dobaradaran, T.C. Schmidt, M. Malakootian, J. Spitz, Emerging contaminants migration from pipes used in drinking water distribution systems: a review of the scientific literature, Environ. Sci. Pollut. Res. 29 (2022) 75134–75160, https://doi.org/10.1007/s11356-022-23085-7.
[15] I. Gambino, F. Bagordo, T. Grassi, A. Panico, A. De Donno, Occurrence of microplastics in tap and bottled water: current knowledge, Int. J. Environ. Res. Public Health 19 (2022) 5283, https://doi.org/10.3390/ijerph19095283.
[16] J. Xue, S.H.-A. Samaei, J. Chen, A. Doucet, K.T.W. Ng, What have we known so far about microplastics in drinking water treatment? A timely review, Front. Environ. Sci. Eng. 16 (2022) 58, https://doi.org/10.1007/s11783-021-1492-5.
[17] W. Tang, H. Li, L. Fei, B. Wei, T. Zhou, H. Zhang, The removal of microplastics from water by coagulation: a comprehensive review, Sci. Total Environ. 851 (2022), 158224, https://doi.org/10.1016/j.scitotenv.2022.158224.
[18] M. Llorca, D. Álvarez-Muñoz, M. Ábalos, S. Rodríguez-Mozaz, L.H.M.L.M. Santos, V.M. León, J.A. Campillo, C. Martínez-Gómez, E. Abad, M. Farré, Microplastics in Mediterranean coastal area: toxicity and impact for the environment and human health, Trends Environ. Anal. Chem. 27 (2020), e00090, https://doi.org/10.1016/j.teac.2020.e00090.
[19] M. Khazali, L. Taghavi, An overview of Persian Gulf environmental pollutions, E3S Web Conf. 325 (2021) 03013, https://doi.org/10.1051/e3sconf/202132503013.
[20] O. Rius-Ayra, A. Biserova-Tahchieva, N. Llorca-Isern, Removal of dyes, oils, alcohols, heavy metals and microplastics from water with superhydrophobic materials, Chemosphere. 311 (2023), 137148, https://doi.org/10.1016/j.chemosphere.2022.137148.
[21] X. Chen, P. Huo, L. Yang, W. Wei, B.-J. Ni, A comprehensive analysis of evolution and underlying connections of water research themes in the 21st century, SSRN Electron. J. 835 (2022), 155411, https://doi.org/10.2139/ssrn.4056858.
[22] N.A. Yaranal, S. Subbiah, K. Mohanty, Identification, extraction of microplastics from edible salts and its removal from contaminated seawater, Environ. Technol. Innov. 21 (2021), 101253, https://doi.org/10.1016/j.eti.2020.101253.
[23] L. Almaiman, A. Aljomah, M. Bineid, F.M. Aljeldah, F. Aldawsari, B. Liebmann, I. Lomako, K. Sexlinger, R. Alarfaj, The occurrence and dietary intake related to the presence of microplastics in drinking water in Saudi Arabia, Environ. Monit. Assess. 193 (2021) 390, https://doi.org/10.1007/s10661-021-09132-9.
[24] R. Pérez-Reverón, J. González-Sálamo, C. Hernández-Sánchez, M. González-Pleiter, J. Hernández-Borges, F.J. Díaz-Peña, Recycled wastewater as a potential source of microplastics in irrigated soils from an arid-insular territory (Fuerteventura, Spain), Sci. Total Environ. 817 (2022), 152830, https://doi.org/10.1016/j.scitotenv.2021.152830.
[25] Z. Kong, M. Huang, X. Fan, Y. Gao, L. Meng, Effect of microplastics on the treatment of high salinity wastewater with antimony by membrane distillation, Huanjing Kexue Xuebao/Acta Sci. Circumstantiae. 41 (2021) 3251–3257, https://doi.org/10.13671/J.HJKXXB.2021.0039.
[26] M. El Batouti, N.F. Alharby, M.M. Elewa, Review of new approaches for fouling mitigation in membrane separation processes in water treatment applications, Separations. 9 (2021) 1, https://doi.org/10.3390/separations9010001.
[27] X.-T. Bui, W. Guo, C. Chiemchaisri, A. Pandey, Current Developments in Biotechnology and Bioengineering: Membrane Technology for Sustainable Water and Energy Management, Elsevier, 2023, https://doi.org/10.1016/C2021-0-03582-3.
[28] E. Drioli, A. Ali, F. Macedonio, Membrane distillation: recent developments and perspectives, Desalination. 356 (2015) 56–84, https://doi.org/10.1016/j.desal.2014.10.028.
[29] E. Nagy, Membrane Distillation, in: Basic Equations Mass Transp. Through a Membr. Layer, Elsevier, 2019, pp. 483–496, https://doi.org/10.1016/B978-0-12-813722-2.00019-4.
[30] A. Alkhudhiri, N. Darwish, N. Hilal, Membrane distillation: a comprehensive review, Desalination. 287 (2012) 2–18, https://doi.org/10.1016/j.desal.2011.08.027.
[31] T. Horseman, Y. Yin, K.S. Christie, Z. Wang, T. Tong, S. Lin, Wetting, scaling, and fouling in membrane distillation: state-of-the-art insights on fundamental mechanisms and mitigation strategies, ACS ES&T Eng. 1 (2021) 117–140, https://doi.org/10.1021/acsestengg.0c00025.
[32] B.A. Sharkh, A.A. Al-Amoudi, M. Farooque, C.M. Fellows, S. Ihm, S. Lee, S. Li, N. Voutchkov, Seawater desalination concentrate — a new frontier for sustainable mining of valuable minerals, Npj Clean Water. 5 (2022) 9, https://doi.org/10.1038/s41545-022-00153-6.
[33] L. Jiang, L. Zhu, L. Chen, Y. Ding, W. Zhang, S. Brice, Coupling hybrid membrane capacitive deionization (HMCDI) with electric-enhanced direct contact membrane distillation (EE-DCMD) for lithium/cobalt separation and concentration, Sep. Purif. Technol. 302 (2022), 122082, https://doi.org/10.1016/j.seppur.2022.122082.
[34] K. Shahid, V. Srivastava, M. Sillanpää, Protein recovery as a resource from waste specifically via membrane technology — from waste to wonder, Environ. Sci. Pollut. Res. 28 (2021) 10262–10282, https://doi.org/10.1007/s11356-020-12290-x.
[35] W. Białas, J. Stangierski, P. Konieczny, Protein and water recovery from poultry processing wastewater integrating microfiltration, ultrafiltration and vacuum membrane distillation, Int. J. Environ. Sci. Technol. 12 (2015) 1875–1888, https://doi.org/10.1007/s13762-014-0557-4.

[36] B. Muster-Slawitsch, N. Dow, D. Desai, D. Pinches, C. Brunner, M. Duke, Membrane distillation for concentration of protein-rich waste water from meat processing, J. Water Process Eng. 44 (2021), 102285, https://doi.org/10.1016/j.jwpe.2021.102285.
[37] M.N. Miranda, M.J. Sampaio, P.B. Tavares, A.M.T. Silva, M.F.R. Pereira, Aging assessment of microplastics (LDPE, PET and uPVC) under urban environment stressors, Sci. Total Environ. 796 (2021), 148914, https://doi.org/10.1016/j.scitotenv.2021.148914.
[38] M.N. Miranda, A.R. Lado Ribeiro, A.M.T. Silva, M.F.R. Pereira, Can aged microplastics be transport vectors for organic micropollutants? – sorption and phytotoxicity tests, Sci. Total Environ. 850 (2022), 158073, https://doi.org/10.1016/j.scitotenv.2022.158073.
[39] PlasticsEurope, Plastics – the facts 2022. https://plasticseurope.org/knowledge-hub/plastics-the-facts-2022/, 2022.
[40] Y. Tong, L. Lin, Y. Tao, Y. Huang, X. Zhu, The occurrence, speciation, and ecological effect of plastic pollution in the bay ecosystems, Sci. Total Environ. 857 (2023), 159601, https://doi.org/10.1016/j.scitotenv.2022.159601.
[41] T.L.S. Silva, S. Morales-Torres, C.M.P. Esteves, A.R. Ribeiro, O.C. Nunes, J. L. Figueiredo, A.M.T. Silva, Desalination and removal of organic micropollutants and microorganisms by membrane distillation, Desalination. 437 (2018) 121–132, https://doi.org/10.1016/j.desal.2018.02.027.
[42] APA. Perfil da Água Balnear - Leça da Palmeira, 2022. Porto, https://apambiente.pt/apa/arh-do-norte.
[43] US-EPA, Surface Water Sampling - Operating Procedure (LSASDPROC-201-R5). https://www.epa.gov/quality/surface-water-sampling, 2021.
[44] B.B. Ashoor, S. Mansour, A. Giwa, V. Dufour, S.W. Hasan, Principles and applications of direct contact membrane distillation (DCMD): a comprehensive review, Desalination. 398 (2016) 222–246, https://doi.org/10.1016/j.desal.2016.07.043.
[45] T.L.S. Silva, S. Morales-Torres, J.L. Figueiredo, A.M.T. Silva, Multi-walled carbon nanotube/PVDF blended membranes with sponge- and finger-like pores for direct contact membrane distillation, Desalination. 357 (2015) 233–245, https://doi.org/10.1016/j.desal.2014.11.025.
[46] G. Rácz, S. Kerker, Z. Kovács, G. Vatai, M. Ebrahimi, P. Czermak, Theoretical and experimental approaches of liquid entry pressure determination in membrane distillation processes, Period. Polytech. Chem. Eng. 58 (2014) 81–91, https://doi.org/10.3311/PPch.2179.
[47] B.J. Holland, J.N. Hay, The thermal degradation of poly(vinyl acetate) measured by thermal analysis–Fourier transform infrared spectroscopy, Polymer (Guildf). 43 (2002) 2207–2211, https://doi.org/10.1016/S0032-3861(02)00038-1.
[48] I. Donelli, G. Freddi, V.A. Nierstrasz, P. Taddei, Surface structure and properties of poly-(ethylene terephthalate) hydrolyzed by alkali and cutinase, Polym. Degrad. Stab. 95 (2010) 1542–1550, https://doi.org/10.1016/j.polymdegradstab.2010.06.011.
[49] W.H. Cobbs, R.L. Burton, Crystallization of polyethylene terephthalate, J. Polym. Sci. 10 (1953) 275–290, https://doi.org/10.1002/pol.1953.120100302.
[50] S.K. Bahl, D.D. Cornell, F.J. Boerio, G.E. McGraw, Interpretation of the vibrational spectra of poly (ethylene terephthalate), J. Polym. Sci. Polym. Lett. Ed. 12 (1974) 13–19, https://doi.org/10.1002/pol.1974.130120103.
[51] A. De Campos, S.M. Martins Franchetti, Biotreatment effects in films and blends of PVC/PCL previously treated with heat, Brazilian Arch. Biol. Technol. 48 (2005) 235–243, https://doi.org/10.1590/s1516-89132005000200010.
[52] M. Schiller, Ö. Aksin Artok, C. Damm, Photopinking of white PVC products: a kind of magic, J. Vinyl Addit. Technol. 24 (2018) 195–207, https://doi.org/10.1002/vnl.21548.
[53] J. Lemaire, N. Siampiringue, R. Chaigneau, P. Delprat, G. Parmeland, P. Dabin, C. Spriet, Towards the prediction of pinking of PVC profiles in mild climatic conditions, J. Vinyl Addit. Technol. 6 (2000) 69–79, https://doi.org/10.1002/vnl.10227.
[54] J. Lemaire, N. Siampiringue, N. Girod, P. Delprat, G. Parmeland, N. Macdonald, C. Spriet, Confirming the pinking mechanism of PVC profiles in mild climatic conditions, J. Vinyl Addit. Technol. 9 (2003) 54–60, https://doi.org/10.1002/vnl.10063.
[55] M. Edge, C.M. Liauw, N.S. Allen, R. Herrero, Surface pinking in titanium dioxide/lead stabiliser filled PVC profiles, Polym. Degrad. Stab. 95 (2010) 2022–2040, https://doi.org/10.1016/j.polymdegradstab. 2010.07.006.
[56] A.L. Andrady. Plastics and the Environment, 2003, https://doi.org/10.1002/0471721557.
[57] The European Parliament and the Council of the European Union, Directive (EU) 2020/2184 on the quality of water intended for human consumption (recast). https://eur-lex.europa.eu/eli/dir/2020/2184/oj, 2020.
[58] A. Barišić, J. Lützenkirchen, G. Lefévre, T. Begović, The influence of temperature on the charging of polytetrafluoroethylene surfaces in electrolyte solutions, Colloids Surf. A Physicochem. Eng. Asp. 579 (2019), 123616, https://doi.org/10.1016/j.colsurfa.2019.123616.
[59] P. Wu, Z. Cai, H. Jin, Y. Tang, Adsorption mechanisms of five bisphenol analogues on PVC microplastics, Sci. Total Environ. 650 (2019) 671–678, https://doi.org/10.1016/j.scitotenv.2018.09.049.
[60] A.K. An, J. Guo, S. Jeong, E.-J. Lee, S.A.A. Tabatabai, T. Leiknes, High flux and antifouling properties of negatively charged membrane for dyeing wastewater treatment by membrane distillation, Water Res. 103 (2016) 362–371, https://doi.org/10.1016/j.watres.2016.07.060.
[61] P. Leroy, A. Lassin, M. Azaroual, L. André, Predicting the surface tension of aqueous 1:1 electrolyte solutions at high salinity, Geochim. Cosmochim. Acta 74 (2010) 5427–5442, https://doi.org/10.1016/j.gca.2010.06.012.
[62] Y. Chen, R. Zheng, J. Wang, Y. Liu, Y. Wang, X.-M. Li, T. He, Laminated PTFE membranes to enhance the performance in direct contact membrane distillation for high salinity solution, Desalination. 424 (2017) 140–148, https://doi.org/10.1016/j.desal.2017.10.007.
[63] H.Z. Syed, R. Hackam, Effects of water salinity, electric stress and temperature on the hydrophobicity of polytetrafluoroethylene, in: 1998 Annu. Rep. Conf. Electr. Insul. Dielectr. Phenom. (Cat. No.98CH36257), IEEE, 1998, pp. 100–103, https://doi.org/10.1109/CEIDP.1998.733865.